OPEN ACCESS
Journal of Innovative Optical Health Sciences
Vol. 15, No. 5 (2022) 2250032 (9 pages)

DOI: 10.1142/S1793545822500328

World Scientific
www.worldscientific.com

Multivariate analysis of serum surface-enhanced Raman spectroscopy of liver cancer patients

Qiwen Wang, Sen Wang, Shengdong Cui, Deyuan Yang, Zheng Huang*,‡ and Shusen Xie†,‡
MOE Key Laboratory of Optoelectronic Science and Technology for Medicine and Fujian Provincial Key Laboratory for Photonics Technology
Fujian Normal University
Fuzhou, Fujian 350007, P. R. China
**huangz@fjnu.edu.cn*
†*ssxie@fjnu.edu.cn*

Received 12 January 2022
Accepted 27 June 2022
Published 12 August 2022

Early diagnosis of liver cancer plays a significant role in reducing its high mortality. In this preliminary study, the feasibility of using serum surface-enhanced Raman spectroscopy (SERS) to identify liver cancer was studied. Serum samples were obtained from liver cancer patients and healthy controls. The differences between the SERS spectra of pre-operation and post-operation of liver cancer patients were also analyzed. The general shape and trend of SERS spectra of health control and liver cancer patients were similar. Multivariate analysis, e.g., PLS-SVM, might be useful for the discrimination of serum SERS spectra of pre-operation and post-operation.

Keywords: Surface-enhanced Raman spectroscopy (SERS); serum; liver cancer; multivariate analysis.

1. Introduction

Liver cancer is a general term for many types of cancer that occur in the liver. Hepatocellular carcinoma (HCC) is the most frequent liver cancer, which accounts for 75% of all the primary liver cancers. HCC is considered the 3rd most common cause of cancer mortalities worldwide.[1] Surgery, medications, and ablation therapy are common treatments of liver cancer. It is recommended that people with high-risk factors of HCC, including chronic Hepatitis B virus infection and dietary exposure to the fungal hepatocarcinogen aflatoxin B1, should receive ultrasound screening for early diagnosis. A pilot study showed that the structural changes in some biomolecules in the blood of liver cancer patients might be detected by surface-enhanced Raman spectroscopy (SERS) and

‡Corresponding authors.

suggested that the serum SERS analysis might offer a noninvisible tool for liver cancer screening.[2]

Raman spectroscopy is a spectroscopic technique, which relies on inelastic scattering of photons that can be determined by vibrational modes of molecules, and therefore, can be used to explore the structural information and identify specific molecules.[3] SERS is a surface-sensitive technique that can enhance Raman scattering by molecules adsorbed on rough metal surfaces.[4] The most commonly used method for performing SERS measurements is to deposit a liquid sample onto a silicon or glass surface with a nanostructured metal layer.[5,6] Such surface enhancement makes SERS suitable for the identification of biomarkers via specific binding of biomolecules and detection of biological fluids by dispersion-enhancing nanoparticles.[7]

Indeed, SERS has been suggested for the biomedical analysis of blood samples and for the noninvasive detection of cancer. For instance, Feng *et al.* suggested that blood plasma SERS analysis might be feasible to identify biomarkers of nasopharyngeal cancer.[8] SERS analysis of blood plasma and serum samples might be used to detect cancers located in the digestive tract.[9–12] The feasibility of using serum SERS analysis to diagnose liver cancer and liver cirrhosis has also been investigated and results suggest that SERS combined with multivariate analysis might improve the diagnostic accuracy.[13,14] Recent studies suggest that the postoperative SERS evaluation of serum proteins might provide a new optical tool for prognostic analysis.[15,16]

In this preliminary study, the feasibility of using SERS to identify biomarkers in the serum of HCC patients was investigated. In addition, serum SERS data obtained before and after operation were also compared using multivariate analysis.

2. Material and Methods

2.1. *Preparation of Ag nanoparticles*

Nano-silver colloids were used as the surface-enhancing substrate and prepared by hydroxylamine hydrochloride reduction method.[17] In brief, 0.017 g of silver nitrate was dissolved in 90 mL of ultrapure water and mixed with hydroxylamine hydrochloride reduction solution, which was prepared by mixing 5 mL of hydroxylamine hydrochloride solution (0.06 mol/L) with 4.5 mL of sodium hydroxide solution (0.1 mol/L). The mixture was continuously stirred until forming milky gray color homogeneous colloid. The colloids were placed in centrifuge tubes and centrifuged at 10000 r/min for 10 min to obtain concentrated silver colloids. The Ag nanoparticle colloids had maximal absorption at 419 nm, average size of 45 ± 6 nm, and concentration of approximately 10^{10} particles/mL.

2.2. *Preparation of serum samples*

Ethical approval for processing the human blood samples was obtained from Fujian Normal University. Blood samples from HCC patients ($n = 25$) before and after surgery and control samples from healthy volunteers ($n = 30$) were provided by the Mengchao Hepatobiliary Hospital (Fuzhou, China). Blood samples were stood at room temperature for 30 min to form clot. The supernatant (including some blood cells and serum) was centrifuged at 1000 rpm for 10 min to separate blood cells and the serum. The serum samples were stored at $-20°$C.

2.3. *SERS measurements*

After thawed at room temperature, 10 μL of serum sample was mixed with an equal volume of silver colloids and transferred to a smooth aluminum sheet. After drying, the SERS spectra were measured using a confocal Raman micro-spectrometer (inVia, Renishaw, UK). A laser beam from 785 nm diode laser ($\sim$ 20 mW) was focused through a Leica objective lens (NA: 0.75, 20×) to excite the samples. A total of three sites were randomly selected from each sample. The SERS spectra were acquired at the range of 400–1800 cm^{-1} under 10 s integration time using WIRE 3.4 software (Renishaw). The SERS measurements were repeated three times for each sample.

2.4. *SERS data analysis*

Vancouver Raman Algorithm was used to remove the autofluorescence background from raw SERS spectra.[18] For each sample, all SERS spectra were normalized to the integrated area under the curve and averaged. Then, the normalized spectra from each group were averaged and used for the analysis and comparison of spectral characteristics of different groups.

2.5. *Multivariate analyses*

Attempt of classification of serum SERS spectra obtained from liver cancer patients before and after operation was made by multivariate analysis. Briefly, a total of 20 samples were randomly selected from pre-operative group and 20 samples from post-operative group for training, and the remaining 10 samples used for testing the classification. For these test samples, the principal components after dimensionality reduction were used as input to the trained model to determine whether the serum was from pre-operative or post-operative group. This process was repeated five times and the results were averaged. The end-to-end open source platform TensorFlow was used for multivariate analysis. The accuracy, sensitivity and specificity of classification were derived from the confusion matrix.[10]

Initially, principal component analysis–linear discriminant analysis (PCA–LDA) was performed. The linear discriminant analysis used dimensionality reduction technique. In addition, several partial least squares (PLS)-based analyses were also conducted after the reduction of dimensionality of SERS spectra. The mean squared error of prediction (MSEP) method was used to determine the minimal number of potential components based on the ratio (e.g., ratio $< 5\%$):

$$(\mathrm{MSEP}_N - \mathrm{MSEP}_{N+1})/\mathrm{MSEP}_N \times 100\%, \quad (1)$$

where N is the number of potential components.

For the partial least square-support vector machine (PLS-SVM) with a Gaussian radial basis function (RBF) analysis, briefly, C-classification was used as the SVM type and RBF as the kernel function. In order to find the best classifier, the optimum parameters of C and γ in the RBF kernel were determined using the grid search method.[19] The search range for C was implemented from 10^0 to 10^3 and that for γ from 10^{-12} to 10^{12}. The SVM performance was expressed as the function of C and γ.

Likewise, the partial least square-discriminant analysis (PLS-DA), partial least square-k-nearest neighbor (PLS-KNN) and partial least square-artificial neural network (PLS-ANN) were also used for the classification analysis of serum SERS spectra of liver cancer patients before and after operation, respectively.

3. Results

3.1. *Comparison of serum SERS spectra of healthy group and liver cancer group*

An initial attempt of this preliminary study was to evaluate the diagnostic potential of SERS spectra of serum samples obtained from liver cancer patients. Figure 1 shows the mean spectra of serum samples of healthy volunteers and liver cancer patients. The main peak position differences between the mean spectra of the normal volunteer serum and the cancer patient serum were reflected at 496, 593, 637, 726, 813, 888, 1137 and 1580 cm^{-1}, respectively. However, the general shape and trend of SERS spectra from the health group and the liver cancer group were too similar to provide for diagnostic purpose, although the majority patients in the liver cancer group suffered from late stage cancer and all required surgical removal of tumor mass.

All tentative attributions of the peaks are summarized in Table 1. According to literatures, those peaks could be attributable to glycogen, phosphatidylinositol, amino acid methionine, C–S (protein), C–C stretching of L-serine, methylene rocking, palmitic acid and C–C stretching of unsaturated compounds, respectively.[20–23] Except for 1580 cm^{-1}, which is classified as C–C stretching of unsaturated compounds, the content of substances assigned by other peak positions in the serum of healthy volunteers

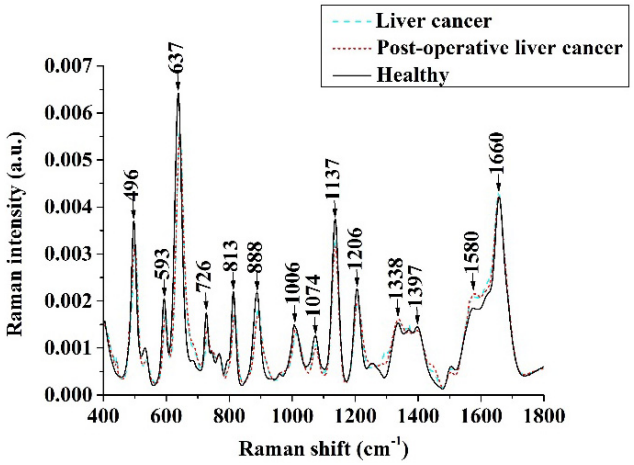

Fig. 1. Serum SERS spectra of heathy volunteers, liver cancer patients and liver cancer patients after operation.

Table 1. SERS peak positions and tentative vibrational mode assignments.

Peak positions (cm^{-1})	Tentative assignments
484	Glycogen
496	Glycogen
507	C–OH_3 torsion of methoxy group
593	Phosphatidylinositol
636	Uric acid
637	Amino acid methionine
725	Hypoxanthine
726	C–S (protein)
813	C–C stretching of L-serine
820	Protein band
888	Methylene rocking
897	Monosaccharides (b-glucose)
1006	Phenylalanine
1074	Fatty acids
1137	Palmitic acid
1146	Glycogen
1206	Tyrosine
1234	A concerted ring mode
1295	CH_2 deformation
1338	Tryptophan
1370	Saccharide band
1397	CH_2 deformation
1445	Collagen
1510	Cytosine
1580	C–C stretching of unsaturated compounds
1625	Tryptophan
1660	Fatty acids
1682	C=O

was higher than that of liver cancer patients. Although nano-Ag-based SERS could identify many important biomolecules in serum samples, the spectral peaks were due to the lack of diagnostic specificity.

3.2. *Comparison of serum SERS spectra before and after operation*

Figure 2 shows the mean spectra of serum samples of liver cancer patients taken before operation and one week after operation. The general shape and trend of serum SERS spectra of two groups were also too similar to be used for discrimination purpose. The peak positions of the difference spectrum between the two groups were mainly reflected by the increase at 484 cm^{-1} and decrease at 507, 1146 and 1295 cm^{-1}, which are attributed to glycogen, C–OH_3 torsion of methoxy group, glycogen and CH_2 deformation, respectively.

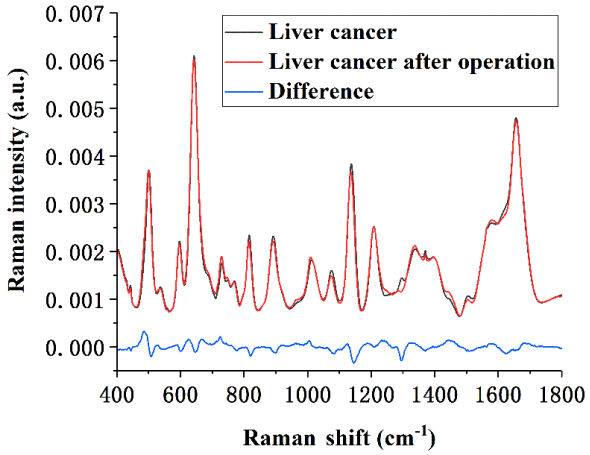

Fig. 2. Spectral difference between serum SERS spectra of liver cancer patients before and after operation.

3.3. *Multivariate analyses of serum SERS spectra obtained before and after operation*

The subtle difference in the mean SERS spectra obtained before and after operation made it difficult to directly discriminate two groups. To test the feasibility of multivariate analysis for the improvement of classification of difference of SERS spectrum between two groups, first, the PCA-LDA model was tested. The first eight principal components, which accounted for 89.4% of the total variance, were used to classify two SERS spectra. The classification accuracy of PCA-LDA analysis was 76% (Table 2).

For PLS-based multivariate analyses, based on MSEP, the 4th component should be excluded from the model, therefore, three principal components were used in the PLS models (Fig. 3).

In this study, SVM was utilized on the three parameters that had the best prediction performance.

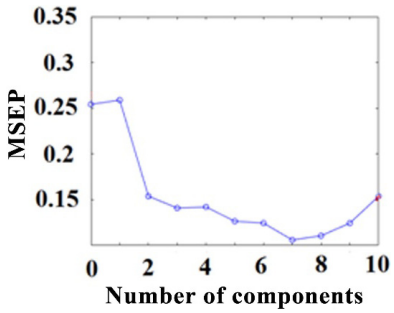

Fig. 3. The relationship between the number of components and the MSEP.

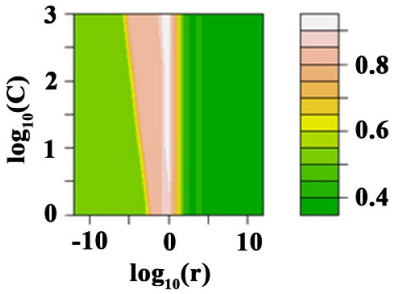

Deeper green color represents worse performance.

Fig. 4. Evaluation of SVM performance as a function of parameters C and γ.

Figure 4 shows the SVM performance as a function of penalty factor C and γ. The optimum C and γ were found to be 10 and 1, respectively. Under this condition, the best classification performance of 97.5% could be obtained from PLS-SVM analysis.

Figure 5 shows the classification results of the RBF kernel SVM model in the feature space from different angles. The pink dots represent serum samples from liver cancer patients before operation, the green dots represent serum samples from liver cancer patients after operation. A gray hyperplane was created in the feature space to distinguish samples obtained before and after the operation. As shown in Fig. 5, the classification of samples obtained before and after the operation could be achieved according to the separating hyperplane obtained by the PLS-SVM training.

Several other classification algorithms, including PLS-DA, PLS-KNN and PLS-ANN, were also evaluated. Two groups of SERS spectra from liver cancer group and post-operative liver cancer group were input in the PLS-DA model for analysis. The PLS-DA model was built using three latent variables. The three latent variables were linear combinations of wavenumbers that represent the spectra changes. The k-Nearest Neighbor (KNN) classification algorithm was also used for the quantitative analysis of the PLS components. In this study, the automatic optimization algorithm was used to determine the k value and the Euclidean distance was selected. According to the results of a series of tests, the best k value was 7. Artificial neural networks (ANN) were also performed for the analysis of the PLS components. Feed-forward networks were chosen for the artificial networks. As ANN is inclined to over-fit, it is best to use the least hidden layers. Therefore, a network with three layers was selected—i.e., an input layer, a hidden layer and an output layer. For the input layer, the first three PLS components were used as inputs. The output layer was the predicted groups that were the liver cancer group and the post-operation group in this case. The hidden layer was composed of an adjustable number of neurons interconnecting input and output layers. According to the results of a series of tests, 11 neurons were used for best performance.

The classification results were summarized in Table 2. PLS-SVM gave the highest accuracy, i.e., 94%. Nonetheless, the overall ranking of classification performance of each algorithm suggested that PLS-SVM was superior to other classification algorithms.

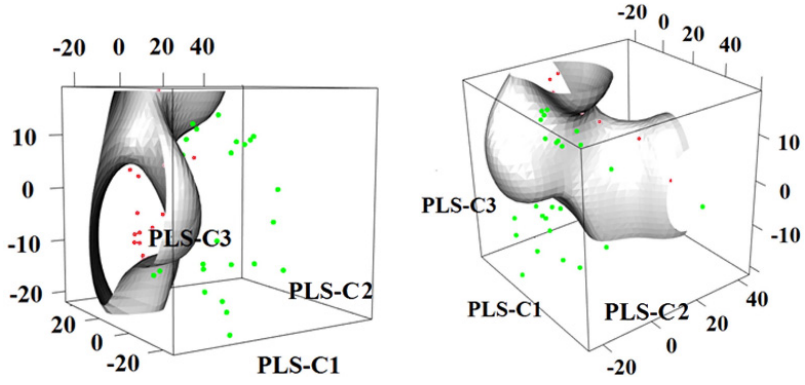

Pink: Samples obtained before operation, green: Samples obtained after operation.

Fig. 5. SVM classification result for the two groups of samples from different angles.

Table 2. Evaluation of algorithms for classification of SERS spectra (rankings are shown in bracket).

Methods	Accuracy	Sensitivity	Specificity	Rank
PLS-SVM	94% (1)	96% (1)	92% (1)	1 (1)
PLS-ANN	92% (2)	96% (1)	88% (4)	2.3 (2)
PLS-KNN	90% (3)	88% (3)	92% (1)	2.3 (2)
PLS-DA	88% (4)	84% (4)	92% (1)	3 (4)
PCA-LDA	76% (5)	76% (5)	76% (5)	5 (5)

4. Discussion

Raman spectroscopy technology is a noninvasive and nondestructive optical tool that can be used to study the spectral profile of biomolecules through vibrational and rotational spectrum information of laser-excited biological specimen. The SERS spectrum of serum has been used to detect the presence of nucleic acids, proteins and lipids. The shape and trend of SERS spectrum might be useful for identifying the changes of these molecular components. Some spectral fingerprints might be linked to specific biomarkers that are useful for the disease diagnosis and classification.[4,7,24] Early studies also suggest that it might be feasible to use serum SERS analysis for the diagnosis of liver cancer.[13,14] This study analyzed SERS spectra of serum samples of 25 HCC patients and 30 healthy adults. Results show that nanoAg-based SERS could identify many important biomolecules in serum samples (see Table 1). However, in terms of the general shape and trend of serum SERS, both spectra were very close and the spectral peaks were lack of the diagnostic specificity (see Fig. 1). This result might suggest that no spectral fingerprints corresponding to specific biomarkers were identifiable for the disease discrimination purpose. It should be noted that the small sample size of health group and the liver cancer group might prohibit accurate SERS spectra classification.

Recent studies suggest that the post-operative SERS evaluation of serum proteins might provide a new optical tool for prognostic analysis of cancer.[15,16] This study analyzed serum SERS spectra obtained from cancer patients before surgery and one week after surgery. Although the overall shape and trend of serum SERS spectra were similar, there were some differences that mainly reflected by the increase at 484 cm^{-1} and decrease at 507, 1146 and 1295 cm^{-1} (see Fig. 2), which are attributed to glycogen, C–OH_3 torsion of methoxy group, glycogen and CH_2 deformation, respectively. However, it was difficult to confirm whether these changes were related to surgical removal of tumor mass. For instance, glycogen metabolism plays a key role in cancer progression, but the post-operative SERS showed both increase and decrease trend of glycogen signals. It was also unclear how blood infusion during operation and post-operation might affect the serum SERS profile. Unfortunately, this study did not collect the blood infusion information.

The small difference made it difficult to directly distinguish the SERS spectra between pre-operative and post-operative groups. To test whether multivariate analysis could improve the classification of difference of SERS spectrum between two groups, several commonly used multivariate analysis algorithms were evaluated.

The principal component analysis is one of the most commonly used statistical methods to simplify spectral datasets and identify key components that best explain spectral differences. LDA is a method to solve the problems of linear discriminant. The classification accuracy of PCA-LDA analysis of pre-operative and post-operative groups was relatively low, i.e., 76% (see Table 2).

The PLS is a supervised linear dimensionality reduction method, which combines the basic principles of principal component analysis, canonical correlation analysis, and linear regression analysis.[10] To assess the performance of PLS-based multivariate analyses, the dimensionality reduction of SERS spectra was conducted in this study in order to choose a suitable number of components to minimize the expected error when predicting the response from future observations on the predictor variables. Simply using a large number of components will do a good job in fitting the current observed data, but such strategy could lead to overfitting. Overfitting the current data results in a model that does not generalize well enough to fit other data, therefore, gives an overly-optimistic estimate of the expected error. Cross-validation is a more statistically sound method for choosing the number of components in PLS. It minimizes overfitting data by not reusing the same data to fit a model and to estimate prediction error. Thus, the estimate of prediction error is not optimistically biased downwards.[25]

The machine learning techniques have been used to analyze high-dimensional SERS data.[26] Previous studies suggest that in terms of recognition

performance, the SVM algorithm is better than that of the other traditional classification algorithms, e.g., ANN, KNN and LDA.[27] In this study, SVM was utilized on the three parameters that had the best prediction performance (see Figs. 4 and 5).

The KNN classification algorithm is one of the simplest machine learning algorithms. The core idea of the KNN algorithm is that if the majority of the k most neighboring samples in a feature space belong to a certain category, the sample also belongs to this category and has the characteristics of the samples on this category. The performance of KNN can be affected by a lot of factors, such as the selection of the k value and the selection of distance measures. In general, the larger the k value, the smaller the effect of noise on the classification and the less obvious the boundary between the classifications. In this study, the Euclidean distance function was used. Using the automatic optimization algorithm, the best k value of 7 was selected from leave-one-out cross validation. This k value is similar to that reported by others. For instance, Zheng *et al.* used the k value of 6 in KNN analysis of serum Raman spectra.[28]

The ANNs are an engineering system that can make intelligent decision-making like human brain by using artificial neurons to simulate the organization and operation mechanism of neural network in human brain. It can classify by adjusting the highly nonlinear topology. By weighting and transmitting input variables between neurons repeatedly, ANN sorts input observations into different outputs. In this study, a network with three layers was selected — i.e., an input layer, a hidden layer and an output layer. For the input layer, the first three PLS components were used as inputs. The output layer was the predicted groups that were the liver cancer group and the post-operation group.

As shown in Table 2, tested multivariate analysis algorithms showed different classification accuracy. The PLS-SVM method gave rise to the highest accuracy. The overall ranking order of classification performance was PLS-SVM > PLS-ANN/PLS-KNN > PLS-DA > PCA-LDA.

It needs to be noted that one of the major limitations of this preliminary study was the sample size. The small sample size of health group and the liver cancer group might prohibit accurate SERS spectra classification. Since no specific SERS spectral markers were found to be responsible for the disease or sample discrimination, the discrimination relied on the multivariate analysis of the whole spectral data. However, the possible overfitting of the classification models may be a potential problem for this application. Although the multivariate analysis might provide a means to distinguish the SERS spectra of pre-operation and post-operation blood samples, the blood infusion during and post-operation might affect the serum SERS profile. However, this uncertainty was not explored in this study.

5. Conclusions

This preliminary study showed that the general shape and trend of SERS spectra of health control and HCC patients were similar. The differences between the SERS spectra of pre-operation and post-operation of liver cancer patients were also not so obvious. Multivariate analysis, e.g., PLS-SVM analysis, might provide a means to distinguish the SERS spectra of pre-operation and post-operation blood samples. Further validation of these findings will be focused on the improvement and optimization of algorithms and the inclusion of large-scale samples.

Conflict of Interest

The authors declare that there is no conflict of interest related to this manuscript.

Acknowledgments

This work was supported by the National Natural Science Foundation of China (No. 61775037), Natural Science Foundation of Fujian Province of China (No. 2019J01270) and Special Funds of the Central Government Guiding Local Science and Technology Development (No. 2020L3008).

Ethics

Serum samples used in this study were randomly selected from physical examination respondents and liver cancer patients of Mengchao Hepatobiliary Hospital (Fuzhou, China). The research described in this study was performed with full institutional ethical approval.

References

1. A. A. Mokdad, A. G. Singal, A. C. Yopp, "Liver cancer," *JAMA* **314**(24), 2701–2701 (2015).
2. X. Li, T. Yang, S. Li, L. Jin, D. Wang, D. Guan, J. Ding, "Noninvasive liver diseases detection based on serum surface enhanced Raman spectroscopy and statistical analysis," *Opt. Exp.* **23**(14), 18361–18372 (2015).
3. Y. Zhang, L. Lin, J. He, J. Ye, "Optical penetration of surface-enhanced micro-scale spatial offset Raman spectroscopy in turbid gel and biological tissue," *J. Innov. Opt. Health Sci.* **14**(4), 2141001 (2021).
4. L. D. Barron, L. Hecht, I. H. McColl, E. W. Blanch, "Raman optical activity comes of age," *Mol. Phys.* **102**(8), 731–744 (2004).
5. C. L. Haynes, A. D. McFarland, R. P. Van Duyne, "Surface-enhanced Raman spectroscopy," *Anal. Chem.* **77**, 338–346 (2005).
6. B. Barbiellini, "Enhancement of Raman scattering from molecules placed near metal nanoparticles," *Low Temp. Phys.* **43**(1), 159–161 (2017).
7. J. M. Reyes-Goddard, H. Barr, N. Stone, "Photodiagnosis using Raman and surface enhanced Raman scattering of bodily fluids," *Photodiagnosis Photodyn. Ther.* **2**(3), 223–233 (2005).
8. S. Feng, R. Chen, J. Lin, J. Pan, G. Chen, Y. Li, M. Cheng, Z. Huang, J. Chen, H. Zeng, "Nasopharyngeal cancer detection based on blood plasma surface-enhanced Raman spectroscopy and multivariate analysis," *Biosens. Bioelectron.* **25**(11), 2414–2419 (2010).
9. D. Lin, S. Feng, J. Pan, Y. Chen, J. Lin, G. Chen, S. Xie, H. Zeng, R. Chen, "Colorectal cancer detection by gold nanoparticle based surface-enhanced Raman spectroscopy of blood serum and statistical analysis," *Opt. Exp.* **19**(14), 13565–13577 (2011).
10. D. Lin, S. Feng, H. Huang, W. Chen, H. Shi, N. Liu, L. Chen, W. Chen, Y. Yu, R. Chen, "Label-free detection of blood plasma using silver nanoparticle based surface-enhanced Raman spectroscopy for esophageal cancer screening," *J. Biomed. Nanotechnol.* **10**(3), 478–484 (2014).
11. X. Li, T. Yang, S. Li, S. Zhang, L. Jin, "Discrimination of rectal cancer through human serum using surface-enhanced Raman spectroscopy," *Appl. Phys. B* **119**(2), 393–398 (2015).
12. H. Ito, N. Uragami, T. Miyazaki, W. Yang, K. Issha, K. Matsuo, S. Kimura, Y. Arai, H. Tokunaga, S. Okada *et al.*, "Highly accurate colorectal cancer prediction model based on Raman spectroscopy using patient serum," *World J. Gastrointest. Oncol.* **12**(11), 1311 (2020).
13. Y. Yu, Y. Lin, C. Xu, K. Lin, Q. Ye, X. Wang, S. Xie, R. Chen, J. Lin, "Label-free detection of nasopharyngeal and liver cancer using surface-enhanced Raman spectroscopy and partial lease squares combined with support vector machine," *Biomed. Opt. Exp.* **9**(12), 6053–6066 (2018).
14. G. Lü, X. Zheng, X. Lü, P. Chen, G. Wu, H. Wen, "Label-free detection of echinococcosis and liver cirrhosis based on serum Raman spectroscopy combined with multivariate analysis," *Photodiagnosis Photodyn. Ther.* **33**, 102164 (2021).
15. X. Liu, X. Lin, Z. Huang, Y. Zhu, M. Peng, X. Jia, S. Weng, Y. Weng, S. Feng, "Screening and postoperative evaluation of breast cancer based on serum proteins analysis using label-free surface-enhanced Raman spectroscopy technology," *Nanosci. Nanotechnol. Lett.* **12**(7), 901–908 (2020).
16. J. Hu, X. Shao, C. Chi, Y. Zhu, Z. Xin, J. Sha, B. Dong, J. Pan, W. Xue, "Surface-enhanced Raman spectroscopy of serum predicts sensitivity to docetaxel-based chemotherapy in patients with metastatic castration-resistant prostate cancer," *J. Innov. Opt. Health Sci.* **14**(4), 2141006 (2021).
17. N. Leopold, B. Lendl, "A new method for fast preparation of highly surface-enhanced Raman scattering (SERS) active silver colloids at room temperature by reduction of silver nitrate with hydroxylamine hydrochloride," *J. Phys. Chem. B* **107**(24), 5723–5727 (2003).
18. J. Zhao, H. Lui, D. I. McLean, H. Zeng, "Automated autofluorescence background subtraction algorithm for biomedical Raman spectroscopy," *Appl. Spectrosc.* **61**(11), 1225–1232 (2007).
19. X. Li, T. Yang, S. Li, D. Wang, Y. Song, K. Yu, "Different classification algorithms and serum surface enhanced Raman spectroscopy for noninvasive discrimination of gastric diseases," *J. Raman Spectrosc.* **47**(8), 917–925 (2016).
20. R. Liu, Y. Xiong, Y. Guo, M. Si, W. Tang, "Label-free and non-invasive BS-SERS detection of liver cancer based on the solid device of silver nanofilm," *J. Raman Spectrosc.* **49**(9), 1426–1434 (2018).
21. L. Shao, A. Zhang, Z. Rong, C. Wang, X. Jia, K. Zhang, R. Xiao, S. Wang, "Fast and non-invasive serum detection technology based on surface enhanced Raman spectroscopy and multivariate statistical analysis for liver disease," *Nanomed. Nanotechnol. Biol. Med.* **14**(2), 451–459 (2018).
22. L. Guo, Y. Li, F. Huang, J. Dong, F. Li, X. Yang, S. Zhu, M. Yang, "Identification and analysis of serum samples by surface-enhanced Raman spectroscopy combined with characteristic ratio method and PCA for gastric cancer detection," *J. Innov. Opt. Health Sci.* **12**(2), 1950003 (2019).

23. M. Tahira, H. Nawaz, M. I. Majeed, N. Rashid, S. Tabbasum, M. Abubakar, S. Ahmad, S. Akbar, S. Bashir, M. Kashif *et al.*, "Surface-enhanced Raman spectroscopy analysis of serum samples of typhoid patients of different stages," *Photodiagnosis Photodyn. Ther.* **34**, 102329 (2021).
24. X. He, C. Ge, X. Zheng, B. Tang, L. Chen, S. Li, L. Wang, L. Zhang, Y. Xu, "Rapid identification of alpha-fetoprotein in serum by a microfluidic SERS chip integrated with Ag/Au nanocomposites," *Sens. Actuat. B. Chem.* **317**, 128196 (2020).
25. A. Oleszko, J. Hartwich, A. Wójtowicz, M. Gąsior-Głogowska, H. Huras, M. Komorowska, "Comparison of FTIR-ART and Raman spectroscopy in determination of VLDL triglycerides in blood serum with PLS regression," *Spectrochim. Acta A Mol. Biomol. Spectrosc.* **183**, 239–246 (2017).
26. C. Chen, L. Yang, H. Li, F. Chen, C. Chen, R. Gao, X. Lv, J. Tang, "Raman spectroscopy combined with multiple algorithms for analysis and rapid screening of chronic renal failure," *Photodiagnosis Photodyn. Ther.* **30**, 101792 (2020).
27. X. Xie, C. Chen, T. Sun, G. Mamati, X. Wan, W. Zhang, R. Gao, F. Chen, W. Wu, Y. Fan *et al.*, "Rapid, non-invasive screening of keratitis based on Raman spectroscopy combined with multivariate statistical analysis," *Photodiagnosis Photodyn. Ther.* **31**, 101932 (2020).
28. X. Zheng, G. Lv, Y. Zhang, X. Lv, Z. Gao, J. Tang, J. Mo, "Rapid and non-invasive screening of high renin hypertension using Raman spectroscopy and different classification algorithms," *Spectrochim. Acta A Mol. Biomol. Spectrosc.* **215**, 244–248 (2019).